Combined Effects of Suction/Injection on MHD Boundary Layer Flow of Nanofluid over a Horizontal Permeable Cylinder with Radiation

Shalini Jain, Dept. of Mathematics & Statistics, Manipal University Jaipur, Rajasthan, India.
E-mail:shalini.jain@jaipur.manipal.edu

Rakesh Choudhary, Dept. of Mathematics & Statistics, Manipal University Jaipur, Rajasthan, India.
E-mail:rakeshchoudhary@muj.manipal.edu

Abstract--- The present work is concerned with MHD boundary layer flow and heat transfer of Ag-water and Al_2O_3-water nanofluid over a horizontal stretching/shrinking cylinder. The investigation is carried out in the presence of suction/injection, heat source, radiation and shape of the nano-particles. The governing momentum and energy equations are transformed into nonlinear differential equations using suitable similarity transformations. These transformed equations are solved numerically using bvp4c Matlab solver. The effects of significant parameters such as nanofluid type, nano-particle volume friction, suction/injection parameter, magnetic field parameter, heat source parameter, radiation parameter on fluid flow and heat transfer are discussed.

Keywords--- MHD, Stretching/Shrinking Cylinder, Nanofluid, Suction/Injection, Heat Source, Radiation.

I. Introduction

Nanofluid is a fluid containing nanometer-sized elements, these elements are called nanoparticles. Nano particles are usually made of metals, oxides, carbides, or carbon nanotubes. Nanofluids have enhanced thermal conductivity and the convective heat transfer coefficient, compared to the base fluid. Nanofluid have many novel properties that make them so reliable in heat transfer processes, such as microelectronics, fuel cells, hybrid-powered engines, engine cooling/vehicle thermal management. The study of stagnation point flow plays a vital role in fluid dynamics. It has many applications such as transpiration, oil recovery, nuclear reactors and production. Firstly, Massoudi and Rameza [1] studied heat transfer analysis of boundary layer flow of a viscoelastic fluid at a stagnation point. Singh and Mittal [2] investigated flow past a cylinder: shear layer instability and Drag crisis. Sami Akoz and Salih Kirkzgoz [3] investigated numerical and experimental analysis of the flow around a horizontal wall-mounted circular cylinder. Bhattacharyya [4] analyzed unsteady boundary layer stagnation-point flow's heat transfer analysis towards a shrinking/stretching sheet. Ashorynejad et al. [5] have examined the Nanofluid flow and heat transfer due to a stretching cylinder in the presence of magnetic field. Dual solutions of mixed convection flow with momentum and thermal slip flow over a permeable shrinking cylinder investigated by Mishra and Singh [6]. Rana and Be´g [7] addressed the mixed convection flow along an inclined permeable plate: effect of magnetic field, nanolayer conductivity and nanoparticle diameter. Pal and Mandal [8] studied effects of hall current on magnetohydro dynamic heat transfer of nanofluids over a non-linear stretching/shrinking sheet. Nanoparticle volume fraction with heat and mass transfer on MHD mixed convection flow in a nanofluid in the presence of thermo-diffusion under convective boundary condition examined by Kandasamy et al. [9]. Naramgari and Sulochana [10] have considered MHD flow over a permeable stretching/shrinking sheet of a nanofluid with suction/injection. Khan and Pop [11] studied boundary-layer flow of a nanofluid past a stretching sheet. Bachok et al. [12] discussed stagnation-point flow over a stretching/shrinking in a nanofluid. Makinde and Aziz [13] visualized the boundary layer flow of a nanofluid past a stretching sheet with convective boundary condition. Bhattacharyya [14] presented the dual solutions in boundary layer stagnation-point flow and mass transfer with chemical reaction past a stretching/shrinking sheet. Makinde and Oluwole [15] studied computational modelling of nanofluids flow over a convectively heated unsteady stretching sheet. Makinde et al. [16] investigated buoyancy effects on MHD stagnation-point flow and heat transfer of a nanofluid past a convectively heated stretching/shrinking sheet. Najib et al. [17] studied stagnation point flow and mass transfer with chemical reaction past a stretching/shrinking cylinder. Rashidi et al. [18] presented Homotopy simulation of nanofluid dynamics from a nonlinearly stretching isothermal permeable sheet with transpiration. Boundary layer flowand heat transfer over a nonlinearly permeable stretching/shrinking sheet in a nanofluid were studied by Zaimi et al. [19]. Effect of double stratification on mixed convection boundary-layer flow of a nanofluid past a vertical plate in a porous medium was examined by Srinivasacharya and Surender [20]. Recently, Mabood et al. [21] studied stagnation point flow of nanofluid over a moving plate with convective boundary condition and magnetohydro dynamics. Sulochana and Sandeep [22] analyzed stagnation-point flow and heat transfer behavior of Cu–water nanofluid towards horizontal and exponentially stretching/ shrinking cylinders.

There are several researchers have done a lot of work in the nanofluid with radiation, such as Sandeep et al. [23] studied effects of radiation on an unsteady natural convective flow of a nanofluid past an infinite vertical plate. Ali et al. [24] studied unsteady stagnation-point flow towards a shrinking sheet with radiation effect. Cortell [25] investigated MHD flow and radiative nonlinear heat transfer of a viscoelastic fluid over a stretching sheet with heat generation/absorption. Mohankrishna et al. [26] examined radiation and magneticfield effects on unsteady natural convection flow of a nanofluid past an infinite vertical plate with heat source. Shateyi and Prakash [27] gave a note on new numerical approach for MHD laminar boundary layer flow and heat transfer of nanofluids over a moving surface in the presence of thermal radiation. Chemical reaction and radiation absorption effects on the flow and heat transfer of a nanofluid in a rotating system studied by Venkateswarlu and Satya Narayana [28]. Pal and Mandal [29] investigated mixed convection-radiation on stagnation point flow of nanofluid over a stretching/shrinking sheet in a porous medium with heat generation and viscous dissipation. Recently, Sandeep and Sulochana [30] discussed dual solutions of radiative MHD nanofluid flow over an exponentially stretching sheet with heat generation/absorption.

Abel and Nandeppanavar [31] examined heat transfer in MHD viscoelastic boundary layer flow over a stretching sheet with non-uniform heat source/sink. Reddy et al. [32] studied effects of chemical reaction, radiation and rotation on MHD nanofluid flow past a permeable flat plate in a porous medium. In recent times, Hsiao [33] examined stagnation electrical MHD nanofluid mixed convection with slip boundary on a stretching sheet.

The present study is focused on a comparative study of shrinking/stretching conditions of the given setup in both suction and injection. This is the extended work of Sulochana and Sandeep [22]. Also, we studied the behavior of Ag-water nanofluid and Al_2O_3-water nanofluid embedded in horizontal stretching/shrinking cylinder.

The governing equations are transformed into ordinary differential equations using some similarity transformation. These equations are solved numerally with the help of bvp4c Matlab package. The effects of the various parameter such as curvature parameter K, magnetic field parameter M, radiation parameter N etc. are examined and presents through suitable graphs and tables.

II. Mathematical Formulation

We have considered a steady stagnation point flow (fig. 1) and heat transfer of Ag-water and Al_2O_3-water nanofluid on R radius based horizontal stretching/shrinking cylinder engaged in an incompressible MHD viscous nanofluid with suction/injection and radiation at a constant temperature T_w.

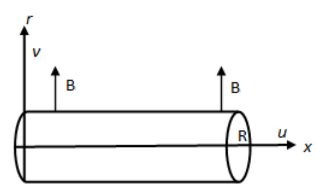

Fig 1: Physical Modal of the Problem

In this study, we have done comparison study in different types of nanoparticles such that Ag-water and Al_2O_3-water. Table I shows the thermo-physical properties of the nanofluid. We have also considered that the free stream and suction/injection velocities are $u_e = ax/L$ and $u_w = cx/L$, where L is a characteristic length and a, c are both constants. Uniform heat source Q is assumed in this study.

Table 1: Thermo-physical Properties of Water and Nanoparticles

Fluids	$\rho(kg\,m^{-3})$	$c_p(J\,kg^{-1}\,K^{-1})$	$k(Wm^{-1}K^{-1})$	$\beta\times10^5(K^{-1})$
H_2O (Pure Water)	997.1	4179	0.613	21
Ag (Silver)	10500	235	429	1.89
Al_2O_3 (Alumina)	3970	765	40	0.85

Under these assumption the governing boundary layer equations followed byc[17] and [21], are:

$$\frac{\partial}{\partial x}(ru)+\frac{\partial}{\partial r}(rv)=0, \tag{1}$$

$$\rho_{nf}\left(u\frac{\partial u}{\partial x}+v\frac{\partial u}{\partial r}\right)=\mu_{nf}\left(\frac{\partial^2 u}{\partial r}+\frac{1}{r}\frac{\partial u}{\partial r}\right)+u_e\frac{\partial u_e}{\partial x}+\sigma_{nf}B_0^2(u_e-u), \tag{2}$$

$$(\rho_{cp})_{nf}\left(u\frac{\partial T}{\partial x}+v\frac{\partial T}{\partial r}\right)=k_{nf}\left(\frac{\partial^2 T}{\partial r^2}+\frac{1}{r}\frac{\partial T}{\partial r}\right)-\frac{\partial q_r}{\partial r}+Q(T-T_\infty), \tag{3}$$

Subject to boundary conditions are as follows:

$$u=u_w,\quad v=v_w,\quad T=T_w,\quad \text{at } r=R \text{ and } u\to u_e,\quad T\to T_\infty \text{ as } r\to\infty \tag{4}$$

where v_w is the suction $(v_w<0)$ and injection $(v_w>0)$ velocity.

Where r is the coordinate measured in the radial direction, u and v are the velocity components in the x and r directions, respectively. ρ_{nf}, μ_{nf} and σ_{nf} are the density, the dynamic viscosity and electrical conductivity of the fluid. B_0 is the imposed magnetic flied strength. Further, T and T_∞ are the temperature in the boundary layer and free stream temperature, respectively, $(\rho_{cp})_{nf}$ is the heat capacitance of nanofluid, k_{nf} is the effective thermal conductivity of the nanofluid, q_r is the radiative heat flux, Q is the heat source parameter, here we assumed $Q=Q_0$ for horizontal cylinder. The radiative heat flux in energy equation is given by Rossel and approximation and is denoted as follows $q_r=-\frac{4\sigma_1}{3k_1}\frac{\partial T^4}{\partial x}$, where σ_1 is the is the Stephan-Boltzmann constant and k_1 is the mean absorption constant. T^4 may be expressed in terms of T is $T^4\cong 4T_\infty^3 T-3T_\infty^4$. The nanofluid constant are as follows [22]

$$\rho_{nf}=(1-\phi)\rho_f+\phi\rho_s,\ (\rho_{cp})_{nf}=(1-\phi)(\rho_{cp})_f+\phi(\rho_{cp})_s,$$

$$\frac{k_{nf}}{k_f}=\left(\frac{k_s+(n-1)k_f-\phi(n-1)(k_f-k_s)}{k_s+(n-1)k_f+\phi(k_f-k_s)}\right),\ \mu_{nf}=\frac{\mu_f}{(1-\phi)^{2.5}}, \tag{5}$$

where n is the nanoparticle shape, $n=3/2$ for cylindrical-shaped nanoparticle and $n=3$ for spherical-shaped nanoparticles (Hamilton and Crosser 1962), ϕ is the volume fraction of the nanoparticle. The subscripts f and s refer to fluid and solid properties, respectively. We introduce the following similarity transformation for Eqs. (1)-(3) with respect to the boundary conditions (Eq. (4))

$$\eta=\frac{r^2-R^2}{2R}\sqrt{\frac{a}{v_f L}},\ \psi=\sqrt{\frac{v_f a}{L}}xR\,f(\eta),\ \theta(\eta)=\frac{T-T_\infty}{T_w-T_\infty}, \tag{6}$$

where η is the similarity variable, ψ is the stream function defined as $u=r^{-1}\partial\psi/\partial r$ and $v=-r^{-1}\partial\psi/\partial x$, these transformations are identically satisfied the Eq. (1). Using Eq. (6), Eqs. (2) and (3) reduces into the nonlinear ordinary differential equations (7) and (8)

$$\frac{1}{(1-\phi)^{2.5}}[(1+2\eta K)f'''+2Kf'']+\left(1-\phi+\phi\left(\frac{\rho_s}{\rho_f}\right)\right)\left(ff''-f'^2\right)+M(1-f')+1=0 \tag{7}$$

$$\frac{1}{Pr}\left(\frac{k_{nf}}{k_f}+\frac{4}{3}N\right)[(1+2\eta K)\theta''+2K\theta']+f\theta'\left(1-\phi+\phi\frac{(\rho_{cp})_s}{(\rho_{cp})_f}\right)+Q_H\theta=0 \tag{8}$$

Subject to boundary conditions:

$$f(0)=S,\ f'(0)=\lambda,\ \theta(0)=1,\ f'(\infty)\to 1,\ \theta(\infty)\to 0, \tag{9}$$

where K is the curvature parameter, Pr is the Prandtl number, N is the radiation parameter, Q_H is the heat source parameter, M is the magnetic field parameter, S is the suction ($S<0$)/ injection ($S>0$) parameter and λ is the stretching/shrinking parameter, here $\lambda>0$ for stretching and $\lambda<0$ shrinking, such as

$$K=\frac{1}{R}\sqrt{\frac{v_f L}{a}},\ Pr=\frac{v_f}{\alpha_f},\ Q_H=\frac{Q_0 L}{a(\rho_{cp})_f},\ M=\frac{\sigma_{nf}B_0^2 L}{a\rho_f}\ N=\frac{4\sigma^1 T_\infty^3}{k^1 k_f},\ S=-v_w\sqrt{\frac{2v_f}{u_w}},\ \ \lambda=\frac{c}{a},\ \ (10)$$

The physical quantities of practical interest, in this study, local skin friction coefficient and local Nusselt number are defined as

$$C_f=\frac{\tau_w}{\rho_f u_e^2},\ Nu=q_r-\frac{xq_w}{k_f(T_w-T_\infty)},\qquad (11)$$

Where τ_w and q_w are the shear stress and heat transfer of the surface of the cylinder. Using Eq. (6) we get

$$\sqrt{Re}C_f=\frac{1}{(1-\phi)^{2.5}}f''(0),\qquad \frac{Nu}{\sqrt{Re}}=-\frac{k_{nf}}{k_f}\left(1+\frac{4N}{3}\right)\theta'(0),\quad (12)$$

Where *Re* is the local Reynolds number.

III.Result and Discussion

Using BVP4c Matlab package equations (7) and (8) are solved numerically with the given boundary conditions (Eq. (9)). We have considered $Pr=6.2$, $\eta=50$, $K=0.5$, $M^2=0.5$, $N=1$, $Q_H=1$, $\lambda=2$, $n=3$ and $S=1$ for numerical results. For whole computational study excluded the varied values as shown in particular figures and table, these values are preserved same.

Numerical results show the variation of the non-dimensional governing parameter such as curvature parameter K, magnetic field parameter *M*, radiation parameter N, suction/injection parameter S, heat source parameter Q_H, shrinking/stretching parameter λ, nanoparticles volume fraction ϕ and shape of the nanoparticles.

In this study, our main aim to study the comparison of shrinking/stretching parameter on magnetic field effect and radiation effect for considered setup. Till now there is no study have been dedicated for this setup.

Table 2 and table 3 depicts the comparison of the present results with the previous results of Bhattacharyya [14], Najib et al. [17] and Sulochana et al. [22]. This comparison shows that present results are very well agreement with the previous results. Also these results verify the validity of the present results.

Table 2: Comparison of the Values of $f''(0)$ for Different Values of λ, when ϕ = 0, K = 0 and M = 0

λ	Bhattacharyya [14]	Najib et al. [17]	Present results
-0.25	1.402240	1.402240	1.402247
-0.50	1.495669	1.495669	1.495630
-0.75	1.489298	1.489298	1.489280
-1.00	1.328816	1.328816	1.328791

Table 3: Comparison of the Values of $f''(0)$ for Different Values of λ and K, when ϕ = 0 and M = 0

λ	Najib et al.[17]	Sulochana et al. [22]	Present result	Najib et al. [17]	Sulochana et al. [22]	Present result
When K = 0.2				When K = 0.4		
-0.25	1.539615	1.539615	1.539560	1.667278	1.667278	1.667283
-0.50	1.670569	1.670569	1.670514	1.830752	1.830752	1.830751
-0.75	1.712534	1.712534	1.712451	1.911938	1.911938	1.911932
-1.00	1.629767	1.629767	1.629724	1.883619	1.883619	1.883601

Figures 2a, 2b, 2c and 2d shows the effects of curvature parameter K and comparison of shrinking/stretching parameter on both velocity profile and temperature profile for Ag-water nanofluid and Al_2O_3-water nanofluid. In figure 2a we compared shrinking/stretching parameter for various values of K when suction is applied.

It is clear that for increasing value of curvature parameter K, velocity profile enhanced for both shrinking and stretching condition. Because when we increase the value of K, the radius of the cylinder increases, this procedure helps in to decrease the contact area of the cylinder, hence velocity boundary layer thickness increases. On the other hand in figure 2b boundary layer thickness increases for stretching condition but for shrinking condition velocity profile decreases hence boundary layer thickness reduces. But in figures, 2c and 2d, due to above reason temperature profile increases with curvature parameter K for both situations. Figure 3a, 3b, 3c and 3d displays the comparison of shrinking/stretching parameter λ and effects of magnetic field parameter for Ag-water nanofluid and Al_2O_3-water nanofluid for both suction/injection on velocity profile and temperature profile. It is clearly seen that for every increasing value of magnetic field parameter M, velocity profile decreases for both the conditions. This is due to Lorentz force, creates a resistive type force, which is slow down the motion of fluid in the velocity boundary layer flow.

Hence velocity boundary layer thickness decreases. Due to the same reason enhanced the thermal boundary layer thickness, hence increase in magnetic field parameter, thermal boundary layer thickness increases. In figures 3a and 3b Ag-water nanofluid show high reduction compare to Al_2O_3-water nanofluid. But in temperature profile (see fig. 3c and 3d) Ag-water nanofluid shows high enhancement. Figure 4a, 4b, 4c and 4d illustrates the comparison of shrinking/stretching parameter λ and effects of nanoparticle fluid friction ϕ in velocity and temperature profile for both Ag-water nanofluid and Al_2O_3-water nanofluid.

It is obvious from figures that improvement in volume friction of nanoparticles decreases the velocity profile for stretching condition and increases for shrinking, also enhances the thickness of thermal boundary layer flow. This is because of an improvement in fluid friction of nanoparticles shrinks the velocity boundary layer thickness appropriate to the friction near the walls.

This reduction is high for Ag-water nanofluid. Similarly, due to above reason helps to improve the thermal conductivity of the flow, hence increases in thermal boundary layer thickness for both cases suction/injection in shrinking and stretching (see figs. 4c and 4d). This hike in temperature profile is high for Ag-water nanofluid.

Figure 5a, 5b and 5c depicts the influence of suction/injection parameter S in velocity and temperature profile for both fluids when shrinking and stretching respectively.

Negative values of S shows suction, and positive values of S indicates injection.

All the graphs shows reduction in velocity boundary layer thickness and thermal boundary layer thickness for increasing value of suction/injection parameter S for both shrinking and stretching. Normally suction/injection parameter S shrinks the velocity and thermal boundary layer thickness.

In velocity boundary layer profile Ag-water nanofluid show more reduction than Al_2O_3-water nanofluid, on the other hand in thermal boundary layer profile Al_2O_3-water nanofluid displays high reduction. Figure 6a, 6b and 6c illustrates the effects of stretching/shrinking parameter λ ιn velocity and temperature profile.

It is observed from figures that an increase in stretching/shrinking parameter λ enhance the velocity boundary layer thickness and reduces the fluid temperature for both suction and injection. Here negative values of λ indicate shrinking of the cylinder while positive value shows stretching of cylinder. Figures 7a and 7b displays the comparison of shrinking/stretching parameter λ and effects of radiation parameter N on both fluids for both injection and suction respectively. We know that higher values of radiation parameter produce heat in the fluid, therefore an increase in radiation parameter N, increases thermal boundary layer thickness for both suction and injection.

Figures 8a and 8b illustrate the comparison in shrinking and stretching and effects of heat source parameter Q_H in temperature profile for both fluids for injection and suction respectively. Generally, we know that heat source parameter enhanced the thermal boundary thickness, hence for increasing values of heat source parameter, increases thermal boundary layer thickness for both conditions. Also it is seen that Ag-water nanofluid shows enhancement than Al_2O_3-water nanofluid.

Figures 9a and 9b depicts the comparison of shrinking and stretching for nanoparticle shapes of the temperature profile for Ag-water nanofluid and Al_2O_3-water nanofluid for suction and injection.

It is clear from the figure that for spherical-shaped nanoparticle's heat transfer enhancement is more than the cylindrical-shaped nanoparticles for both fluids on suction and injection.

Table 4: Variation in Skin Friction Coefficient for Different Values of K, M, S and λ when $\phi = 0.1$

K	M	S	λ	$\frac{1}{(1-\phi)^{2.5}} f''(0)$ Ag -Water	$\frac{1}{(1-\phi)^{2.5}} f''(0)$ Al_2O_3 -Water
0.5	0.5	1	2	-3.431488	-2.517434
1.0	0.5	1	2	-2.758716	-2.059196
1.5	0.5	1	2	-2.375902	-1.796064
0.5	0.0	1	2	-3.401163	-2.442839
0.5	0.5	1	2	-3.431488	-2.517434
0.5	1.5	1	2	-3.506016	-2.655932
0.5	0.5	-1	2	-2.199751	-1.779434
0.5	0.5	0	2	-2.759044	-2.120651
0.5	0.5	1	2	-3.431888	-2.517434
0.5	0.5	1	-0.5	2.395237	2.250620
0.5	0.5	1	0.0	1.627727	1.603119
0.5	0.5	1	0.5	0.626112	0.778909

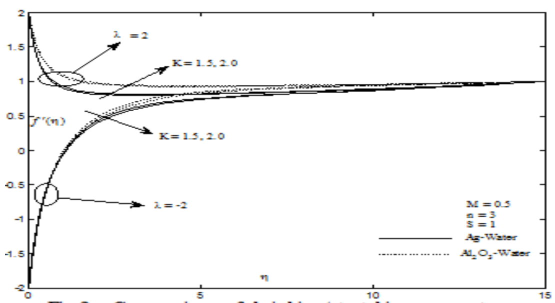

Fig 2a: Comparison of shrinking/stretching parameter when S=1 on velocity profile for K.

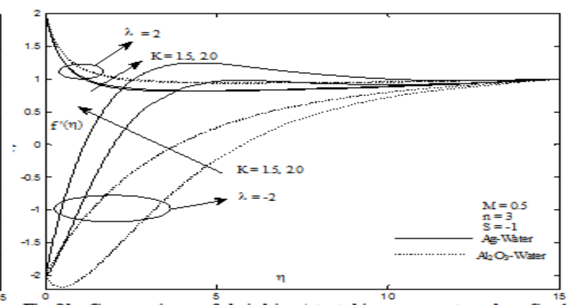

Fig 2b: Comparison of shrinking/stretching parameter when S=-1 on velocity profile for K.

Table 5: Variation Rate of Heat Transfer for Different Values of K, M, S, λ, N, Q_H and n when $\phi = 0.1$ and Pr = 6.2

K	M	S	λ	N	Q_H	n	$-\frac{k_{nf}}{k_f}\left(1+\frac{4N}{3}\right)\theta'(0)$ Ag -Water	$-\frac{k_{nf}}{k_f}\left(1+\frac{4N}{3}\right)\theta'(0)$ Al_2O_3 -Water
0.5	0.5	1	2	1	1	3	4.573741	4.984970
1.0	0.5	1	2	1	1	3	3.188630	3.575913
1.5	0.5	1	2	1	1	3	2.516761	2.863471
0.5	0	1	2	1	1	3	4.580337	4.995910
0.5	0.5	1	2	1	1	3	4.573741	4.984970
0.5	1.5	1	2	1	1	3	4.569003	4.962449
0.5	0.5	-1	2	1	1	3	-3.538511	-1.887805
0.5	0.5	0	2	1	1	3	0.681021	1.336262
0.5	0.5	1	2	1	1	3	4.573741	4.984970
0.5	0.5	1	-0.5	1	1	3	-2.069273	-1.070224
0.5	0.5	1	0.0	1	1	3	0.950374	1.501143
0.5	0.5	1	0.5	1	1	3	2.379429	2.832423
0.5	0.5	1	2	1	1	3	4.573741	4.984970
0.5	0.5	1	2	2	1	3	4.079986	4.658068
0.5	0.5	1	2	3	1	3	3.746975	4.482218
0.5	0.5	1	2	1	0.5	3	5.112646	6.059801
0.5	0.5	1	2	1	1.0	3	4.573741	4.984970
0.5	0.5	1	2	1	1.5	3	3.264644	3.527586
0.5	0.5	1	2	1	1	0	4.023564	4.132654
0.5	0.5	1	2	1	1	3/2	4.486545	4.569878
0.5	0.5	1	2	1	1	3	4.573741	4.984970

Table 4 and 5 shows the variation of skin friction coefficient and rate of heat transfer for different parameters such as curvature parameter K, magnetic field parameter M, suction/injection parameter S, stretching/shrinking parameter λ, radiation parameter N, heat source parameter Q_H and nanoparticles shaped n when $\phi = 0.1$ and Pr = 6.2

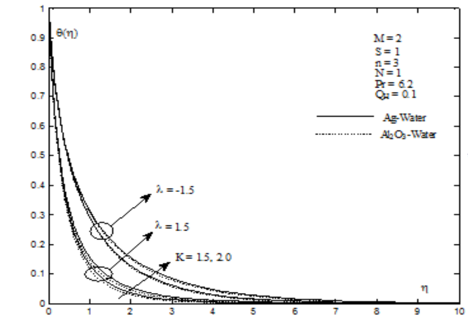

Fig 2c: Comparison of shrinking/stretching parameter when S=1 on temperature profile for K

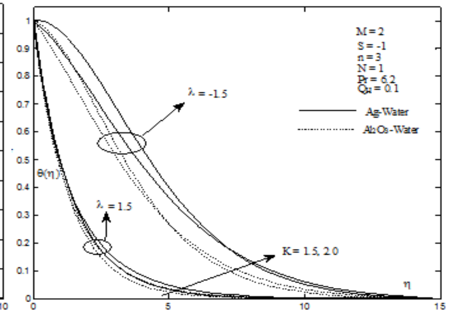

Fig 2d: Comparison of shrinking/stretching parameter when S=-1 on temperature profile for K

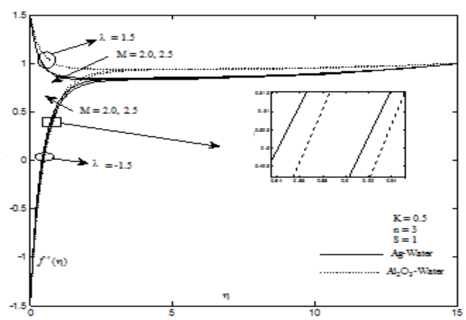

Fig 3a: Comparison of shrinking/stretching parameter when S=1 on velocity profile for M.

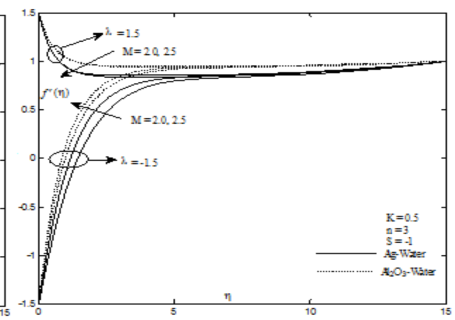

Fig 3b: Comparison of shrinking/stretching parameter when S=-1 on velocity profile for M.

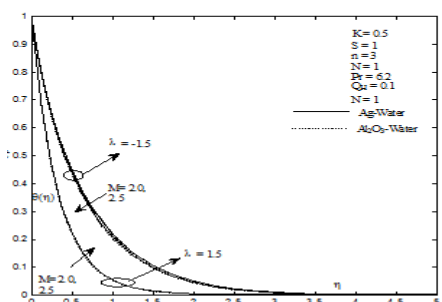

Fig 3c: Comparison of shrinking/stretching parameter when S=-1 on temperature profile for M

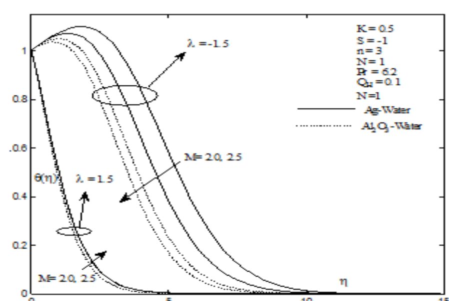

Fig 3d: Comparison of shrinking/stretching parameter when S=-1 on temperature profile for M

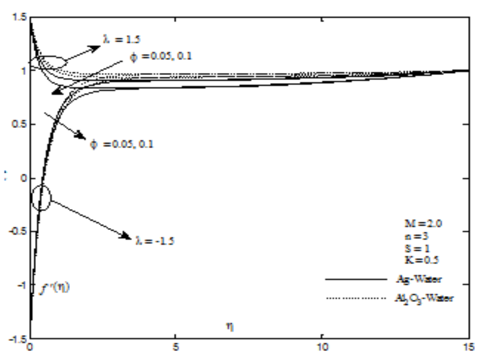

Fig 4a: Comparison of shrinking/ stretching parameter when S=1 on velocity profile for ϕ

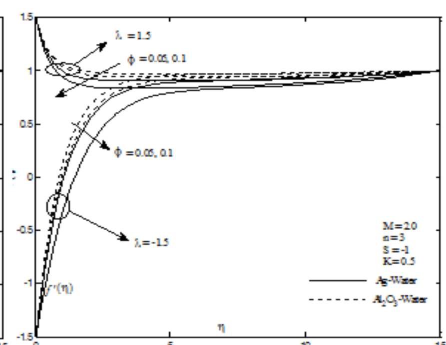

Fig 4b: Comparison of shrinking/stretching parameter when S=-1 on velocity profile for ϕ

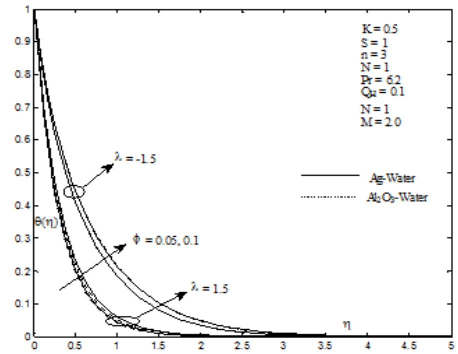

Fig 4c: Comparison of shrinking/stretching parameter when S=1 on temperature profile for ϕ

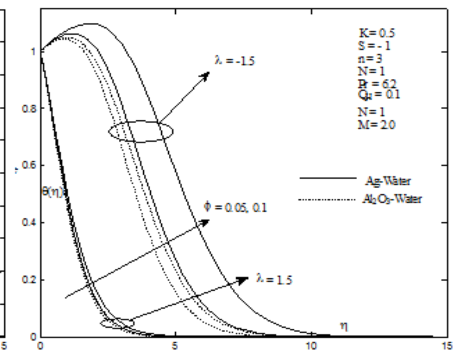

Fig 4d: Comparison of shrinking/stretching parameter when S=-1 on temperature profile for ϕ

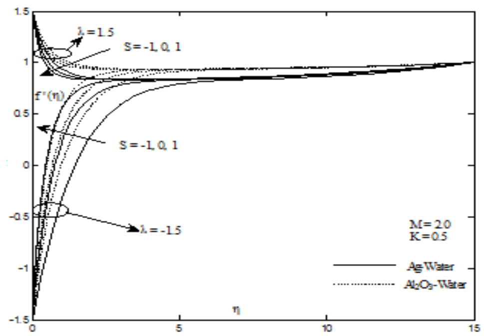

Fig 5a: Comparison of shrinking/stretching parameter on velocity profile for S.

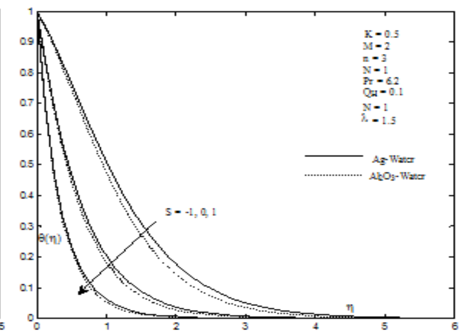

Fig 5b: Influence of suction/injection parameter when λ = 1.5 on temperature profile

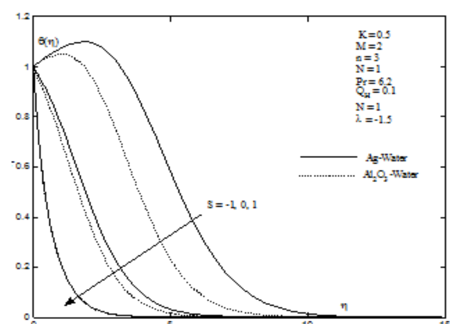

Fig 5c: Influence of suction/injection parameter when λ = -1.5 on temperature profile

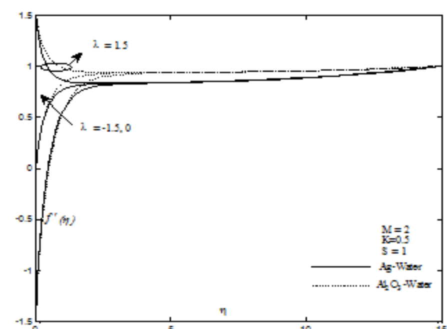

Fig 6a: Influence of shrinking/stretching parameter when S=1 on velocity profile

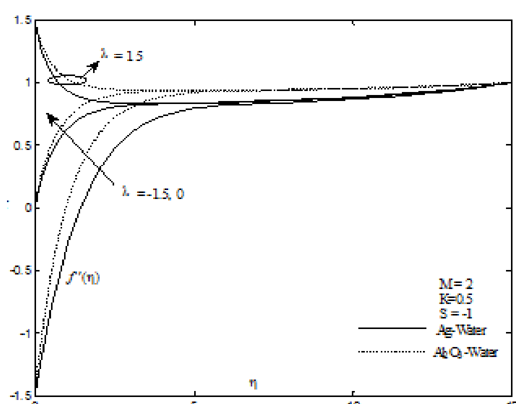

Fig 6b: Influence of shrinking/stretching parameter when S=-1 on velocity profile

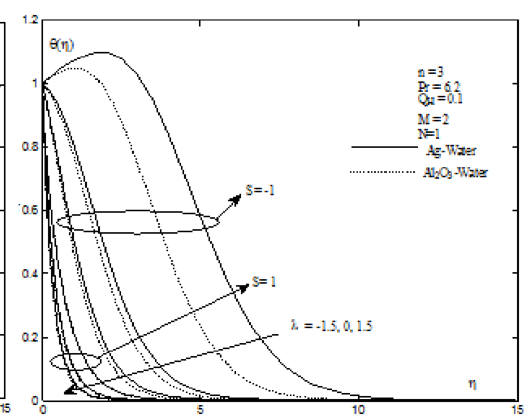

Fig 6c: Influence of shrinking/stretching parameter on temperature profile

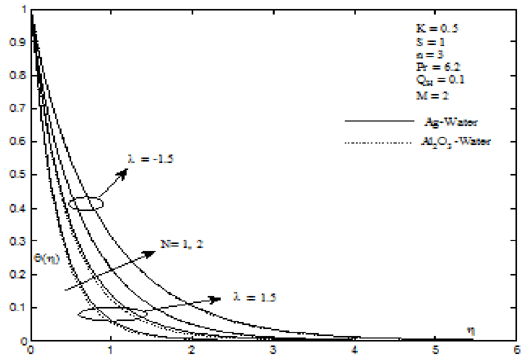

Fig 7a: Comparison of shrinking/stretching parameter when S=1 on temperature profile for N

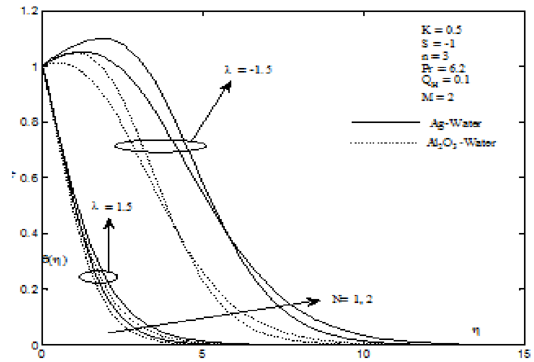

Fig 7b: Comparison of shrinking/stretching parameter when S=-1 on temperature profile for N

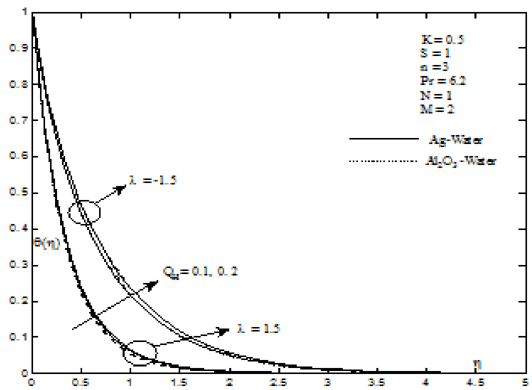

Fig 8a: Comparison of shrinking/stretching parameter when S=1 on temperature profile for Q_H

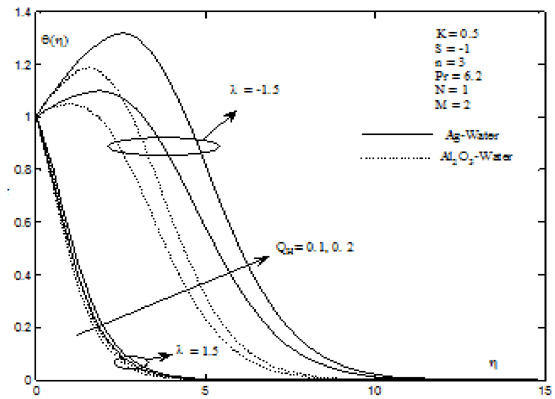

Fig.8b. Comparison of shrinking/stretching parameter when S= -1 on temperature profile for Q_H

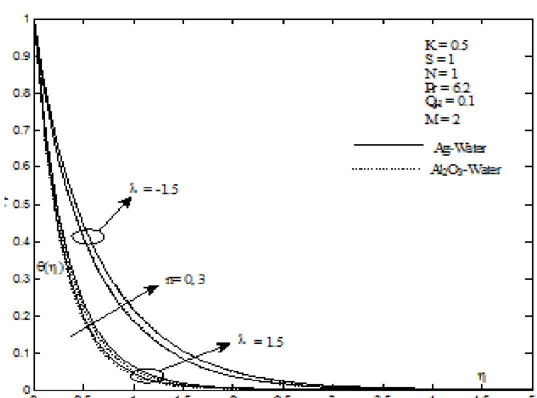

Fig 9a: Comparison of shrinking/stretching parameter when S=1 on temperature profile for n

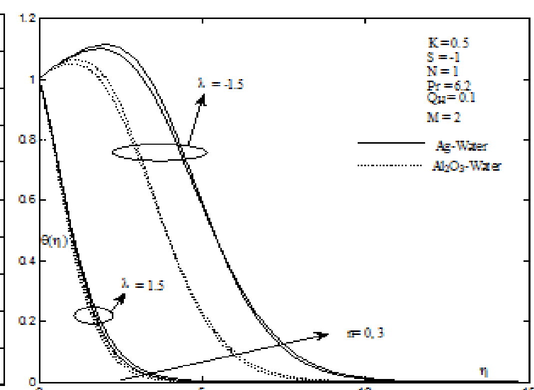

Fig 9b: Comparison of shrinking/stretching parameter when S= -1 on temperature profile for n

IV. Conclusion

The present study, we have investigated the combined effects of suction/injection on MHD boundary layer flow of nanofluid over a horizontal permeable cylinder with radiation. We have also compared the shrinking and stretching condition for this setup. Influence of various parameters such as curvature parameter K, magnetic field parameter M, suction/injection parameter S, shrinking/stretching parameter λ, radiation parameter N and heat source parameter Q_H are examined and displays through suitable graphs and tables. Some important results are as follows: (a) An increment in magnetic field parameter M, causes velocity boundary layer thickness decreases, whereas thermal boundary layer thickness increases for both suction/injection and shrinking/stretching conditions.

(b) When we increase radiation parameter N and heat source parameter Q_H , thermal boundary layer thickness shows enhancement for both conditions.

Acknowledgement

The support provided by Manipal University Jaipur through Endowment Fund Fellowship to one of the authors Rakesh Choudhary is gratefully acknowledged.

References

[1] Massoudi, M. and Rameza, M. Boundary layer heat transfer analysis of a viscoelastic fluid at a stagnation point. *ASME J Heat Transf.,* **130** (1990) 81–86.

[2] Singh, S.P. and Mittal, S. Flow past a cylinder: shear layer instability and Drag crisis. *Int J Numer Meth Fluids* **47** (2005) 75–98.

[3] Sami Akoz, M. and Salih Kirkzgoz, M. Numerical and experimental analysis of the flow around a horizontal wall-mounted circular cylinder. *Trans Can Soc Mech Eng.* **33** (2) (2009) 189–215.

[4] Bhattacharyya, K. Heat transfer analysis in unsteady boundary layer stagnation-point flow towards a shrinking/stretching sheet. *Ain Shams Eng J.* **4** (2) (2013) 259–264.

[5] Ashorynejad, H.R., Sheikholeslami, M., Pop, I. and Ganji, D.D. Nanofluid flow and heat transfer due to a stretching cylinder in the presence of magnetic field. *Heat Mass Transfer* **49** (2013) 427–436

[6] Mishra, U. and Singh, G. Dual solutions of mixed convection flow with momentum and thermal slip flow over a permeable shrinking cylinder. *Comp Fluids.* **93** (2014) 107–115.

[7] Rana, P. and Be´g, O.A. Mixed convection flow along an inclined permeable plate: effect of magnetic field, nanolayer conductivity and nanoparticle diameter. *Appl Nanosci.* **5** (2015) 569–581.

[8] Pal, D. and Mandal, G. Effects of Hall Current on Magnetohydro dynamic Heat Transfer of Nanofluids over a Non-linear Stretching/Shrinking Sheet, *Int. J. Appl. Comput*. **3** (2) (2017) 1103-1120.

[9] Kandasamy, R., Jeyabalan, C. and Prabhu, K.K.S. Nanoparticle volume fraction with heat and mass transfer on MHD mixed convection flow in a nanofluid in the presence of thermo-diffusion under convective boundary condition. *Appl Nanosci.* **6** (2016) 287–300.

[10] Naramgari, S. and Sulochana, C. MHD flow over a permeable stretching/shrinking sheet of a nanofluid with suction/injection. *Alexandria Engineering Journal* **55** (2016) 819–827.

[11] Khan, W.A. and Pop, I. Boundary-layer flow of a nanofluid past a stretching sheet. *Int J Heat Mass Trans* **53** (2010) 2477–2483.

[12] Bachok, N., Ishak, A. and Pop, I. Stagnation-point flow over a stretching/shrinking in a nanofluid. *Nano Scale Res lette.* **6** (2011) 623–630.

[13] Makinde, O.D. and Aziz, A. Boundary layer flow of a nanofluid past a stretching sheet with convective boundary condition. *Int J Ther Sci.* **50** (2011) 1326–1332.

[14] Bhattacharyya, K. Dual solutions in boundary layer stagnation-point flow and mass transfer with chemical reaction past a stretching/shrinking sheet. *Int. Commun. Heat Mass Trans.* **38** (2011) 917–922.

[15] Daniel Makinde, O. Computational Modelling of nanofluids flow over a convectively heated unsteady stretching sheet. *Curr Nanosci.* **9** (5) (2013) 673–678.

[16] Makinde, O.D., Khan, W.A. and Khan, Z.H. Buoyancy effects on MHD stagnation point flow and heat transfer of a nanofluid past a convectively heated stretching/shrinking sheet. *Int J Heat Mass Transf.* **62** (2013) 526–533.

[17] Najib, N., Bachok, N., Arifin, M.D. and Ishak, A. Stagnation point flow and mass transfer with chemical reaction past a stretching/shrinking cylinder. *Sci Rep* **4** (2014).

[18] Rashidi, M.M., Freidoonimehr, N., Hosseini, A., Anwar Beg, O. and Hung, T.K. Homotopy simulation of nanofluid dynamics from a nonlinearly stretching isothermal permeable sheet with transpiration. *Mechanica* **49** (2) (2014) 469–482.

[19] Zaimi, K., Ishak, A. and Pop, I. Boundary layer flow and heat transfer over a nonlinearly permeable stretching/shrinking sheet in a nanofluid. *Scientific reports* (2014)

[20] Srinivasacharya, D. and Surender, O. Effect of double stratification on mixed convection boundary layer flow of a nanofluid past a vertical plate in a porous medium. *Appl Nanosci.* **5** (2015) 29–38.

[21] Mabood, F., Pochai, N. and Shateyi, S. Stagnation Point Flow of Nanofluid over a Moving Plate with Convective Boundary Condition and Magnetohydro dynamics. *Journal of Engineering.*

[22] Sulochana, C. and Sandeep, N. Stagnation point flow and heat transfer behavior of Cu–water nanofluid towards horizontal and exponentially stretching/shrinking cylinders. *Appl Nanosci.* **6** (2016) 451–459.
[23] Sandeep, N., Sugunamma, V. and Mohankrishna, P. Effects of radiation on an unsteady natural convective flow of a nanofluid past an infinite vertical plate. *Adv Phys Theor Appl* **23** (2013) 36–43.
[24] Ali, F.M., Nazar, R., Arifin, N.M. and Pop, I. Unsteady stagnation-point flow towards a shrinking sheet with radiation effect. *Int J Math Comp Natural Phy Eng.* **8** (5) (2014) 751–755.
[25] Cortell, R. MHD (magneto-hydro dynamic) flow and radiative nonlinear heat transfer of a viscoelastic fluid over a stretching sheet with heat generation/absorption. *Energy*. **74** (2014) 896–905
[26] Mohankrishna, P., Sugunamma, V. and Sandeep, N. Radiation and magneticfield effects on unsteady natural convection flow of a nanofluid past an infinite vertical plate with heat source. *Chem Process Eng Res.* **25** (2014) 39–52.
[27] Shateyi, S. and Prakash, J. A new numerical approach for MHD laminar boundary layer flow and heat transfer of nanofluids over a moving surface in the presence of thermal radiation. *Boundary Value Problems* (2014).
[28] Venkateswarlu, B. and Satya Narayana, P.V. Chemical reaction and radiation absorption effects on the flow and heat transfer of a nanofluid in a rotating system. *Appl Nanosci.* **5** (2015) 351–360.
[29] Pal, D. and Mandal, G. Mixed convection-radiation on stagnation point flow of nanofluid over a stretching/shrinking sheet in a porous medium with heat generation and viscous dissipation. *J Petro Sci Eng.* **126** (2015) 16–25.
[30] Sandeep, N. and Sulochana, C. Dual solutions of radiative MHD nanofluid flow over an exponentially stretching sheet with heat generation/absorption. *Appl Nanosci.* **6** (2016) 131–139.
[31] Abel, M.S. and Nandeppanavar, M.M. Heat transfer in MHD viscoelastic boundary layer flow over a stretching sheet with non-uniform heat source/sink. *Int J Commu Nonlinear Sci Numer Simul.***14** (2009) 2120–2131.
[32] Reddy, J.V.R., Sugunamma, V., Sandeep, N. and Sulochana, C. Influence of chemical reaction, radiation and rotation on MHD nanofluid flow past a permeable flat plate in porous medium. *Journal of the Nigerian Mathematical Society* **35** (2016) 48–65.
[33] Hsiao, K.L. Stagnation electrical MHD nanofluid mixed convection with slip boundary on a stretching sheet. *Applied Thermal Engineering* **98** (2016) 850–861.

Dr. Shalini Jain, Professor, Department of Mathematics and Statistics, is presently working in Manipal University. I was born and brought in district Jaipur, Rajasthan, India. In the journey of teaching and learning,I completed my M.Sc., M Phil. and Ph. D. in Mathematics from the University of Rajasthan. Since then, I have a progressive career of sixteen years in teaching math. I have performed well as a faculty member and have a keen interest in research. Research paper publication and presentation is a quest for more and more and deeper knowledge of my subject area. I have published several research papers in good journals of reputed including which includes Procedia Engineering (Elsevier), Int. Journal of Energy and Technology (USA).Supervising Research Scholars.

Rakesh Choudhary, was born and brought up in district Jaipur, Rajasthan, India. I have done my B.Sc. (PCM) from University Maharaja College, Jaipur in 2012 and M.Sc. (Mathematics) from Manipal University Jaipur in 2014. Presently I am perusing my Ph.D. from Manipal University Jaipur in Fluid Dynamics and working as teaching assistant/Research Scholar in Manipal University Jaipur. I have attended a number of national and international conferences & presented papers. I have published research papers in journals including Global and Stochastic Analysis and Procedia Engineering (Elsevier).